KYBERNETIKA — VOLUME 43 (2007), NUMBER 6, PAGES 831 – 840

APPLICATION OF A MULTIPHASE FLOW CODE FOR INVESTIGATION OF INFLUENCE OF CAPILLARY PRESSURE PARAMETERS ON TWO-PHASE FLOW

Jiří Mikyška and Tissa H. Illangasekare

We have developed a multiphase flow code that has been applied to study the behavior of non-aqueous phase liquids (NAPL) in the subsurface. We describe model formulation, discretization, and use the model for numerical investigation of sensitivity of the NAPL plume with respect to capillary parameters of the soil. In this paper the soil is assumed to be spatially homogeneous. A 2-D reference problem has been chosen and has been recomputed repeatedly with modified parameters of the Brooks–Corey capillary pressure model. In this paper we present selected figures showing the resulting plumes as well as quantitative information regarding position of the center of mass of the plume and variances (spreads) of the plume in both axes. These data allow us to evaluate influence of the capillary pressure parameters on the plume morphology in a way that has already been used for characterization of the plume distribution in laboratory experiments. Results confirm the hypothesis that capillary pressure parameters are the key quantities that determine the fate of organic contaminants in the subsurface, and emphasize the significance of the residual NAPL saturation for correct modeling of the NAPL contamination.

Keywords: two-phase flow, non-aqueous phase liquids (NAPL), control volume finite elements, capillary pressure parameters, Brooks–Corey model, plume sensitivity

AMS Subject Classification: 65M60, 76S05, 76T99

1. INTRODUCTION

Models of two-phase flow, such as described e. g. in [13, 17], are used when solving soil contamination problems by non-aqueous phase liquids (NAPL's). At first, the models are tested on simplified problems with known analytical solutions to verify the correct function of the model. The verified code needs then be calibrated when one desires to use it for solving a more complex problem. As typically not all data involved in the model are known, or are known only with limited accuracy, one has to estimate the missing data or work with approximate values of parameters. A natural question arises, how much does a change in input data of the model affect the resulting contamination plume? Or in other words, how sensitive is the plume on changes of a certain parameter? Information of this kind is important not only when calibrating a model or when using a model with uncertain data but also when

preparing a laboratory experiment or a field test, because, to get meaningful results, the most sensitive parameters must be measured most precisely.

The aim of this paper is to investigate the sensitivity of NAPL contamination plume in a homogeneous medium on changes of capillary pressure parameters. In Sections 2 and 3, we briefly describe the model and the numerical scheme used respectively. In Section 4 we choose a reference problem, whose capillary pressure parameters are perturbed within the range of $-50\,\%$ up to $+50\,\%$ with respect to their reference values. Selected resulting plumes are shown and the quantitative results include the positions of the center of mass and variances (spreads) of the plume.

2. MODEL DESCRIPTION

Let $\Omega \subset \mathbb{R}^d, d = 2$ or 3 be a bounded domain with its boundary denoted as Γ, and $I = \langle 0, T\rangle$ be a finite time interval. In the two-phase flow problem we are required to find functions p_α (phase pressures) and S_α (phase saturations) defined on $\overline{\Omega} \times I$ for $\alpha \in \{w, n\}$ which are solutions to the following system of differential-algebraic equations:

$$\frac{\partial(\phi\rho_\alpha S_\alpha)}{\partial t} - \nabla \cdot \left(\rho_\alpha \frac{k_{r\alpha}(S_\alpha)}{\mu_\alpha} \boldsymbol{K} \left(\nabla p_\alpha - \rho_\alpha \vec{g}\right)\right) = \rho_\alpha q_\alpha, \qquad \alpha \in \{w, n\} \tag{1a}$$

$$S_w + S_n = 1, \tag{1b}$$

$$p_c \equiv p_n - p_w = p_c(S_w), \tag{1c}$$

where ϕ denotes the medium porosity, ρ_α is the α-phase density, μ_α denotes the α-phase viscosity, K is the second-order symmetric positive tensor of the medium permeability (at full saturation), $k_{r\alpha}$ stands for the coefficient of relative permeability of the α-phase, $\vec{g}$ denotes the vector of gravity acceleration and q_α describes the volumetric influx of the α-phase into the domain Ω due to outer sources/sinks. $\alpha \in \{w, n\}$ is the phase index, w denoting the wetting phase (water) and n denoting the non-wetting phase (NAPL). Finally, p_c is the capillary pressure–saturation curve. The solutions is subject to the initial conditions

$$p_\alpha(x, 0) = p_{\alpha 0}(x) \qquad \forall\, x \in \Omega \text{ and } \alpha \in \{w, n\}, \tag{2a}$$

$$S_\alpha(x, 0) = S_{\alpha 0}(x) \qquad \forall\, x \in \Omega \text{ and } \alpha \in \{w, n\}, \tag{2b}$$

and boundary conditions

$$p_\alpha(x, t) = p_{\alpha D}(x, t) \qquad \forall\, (x, t) \in \Gamma_D^{p_\alpha} \times I \text{ and } \alpha \in \{w, n\}, \tag{3a}$$

$$S_\alpha(x, t) = S_{\alpha D}(x, t) \qquad \forall\, (x, t) \in \Gamma_D^{S_\alpha} \times I \text{ and } \alpha \in \{w, n\}, \tag{3b}$$

$$(\rho_\alpha v_\alpha \cdot \vec{n})(x, t) = \phi_\alpha(x, t) \qquad \forall\, (x, t) \in \Gamma_N^{\phi_\alpha} \times I \text{ and } \alpha \in \{w, n\}. \tag{3c}$$

In these equations $\Gamma_D^{p_\alpha}, \Gamma_D^{S_\alpha}$ and $\Gamma_N^{\phi_\alpha}$ denote Dirichlet and Neumann parts of the boundary $\Gamma \equiv \partial\Omega$. Note that generally different boundary decompositions into Dirichlet and Neumann parts are allowed for both phases. It is also assumed that

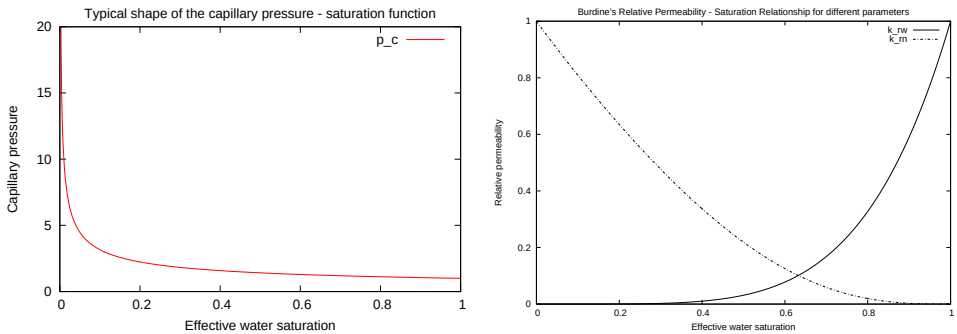

Fig. 1. Typical shape of the capillary pressure – saturation curve (left) and the relative permeabilities – saturation curves (right) as given by the model of Brooks and Corey for a typical water – dense non-aqueous phase liquid (DNAPL) system.

the initial conditions (2a), (2b) and the boundary conditions (3a), (3b), (3c) are compatible with the algebraic constraints (1b) and (1c).

The functions $k_{r\alpha}$ and p_c are non-linear functions of saturations described by the Brooks–Corey model that reads as (e. g. [8, 10, 13, 17])

$$p_c(S_w) = p_d \cdot \left(\overline{S_w}\right)^{-\frac{1}{\lambda}}, \tag{4a}$$

$$k_{rw}(S_w) = \overline{S_w}^{\frac{2+3\lambda}{\lambda}}, \tag{4b}$$

$$k_{rn}(S_n) = \overline{S_n}^2 \left(1 - (1 - \overline{S_n})^{\frac{2+\lambda}{\lambda}}\right), \tag{4c}$$

where the value $p_d \equiv p_c(S_w = 1) > 0$ is called the entry pressure, λ denotes the pore size distribution index and $\overline{S_\alpha}$ is the effective α-phase saturation that is obtained from S_α (α-phase saturation) in terms of the following formula

$$\overline{S_\alpha} = \frac{S_\alpha - S_{\alpha r}}{1 - \sum\limits_{\alpha} S_{\alpha r}}, \tag{5}$$

in which the $S_{\alpha r}$ denote the residual α-phase saturations. In this paper we will study the influence of the entry pressure p_d, pore size distribution index λ, and non-aqueous phase residual saturation S_{nr} on the morphology of contamination plume in the subsurface.

3. NUMERICAL SCHEME

Our numerical technique is based on a weak formulation of the two-phase flow equations in p_w–S_n formulation. Multiplying the equations (1a) by a weighting function W, integrating the equations over Ω, applying Green's theorem, and substituting

the Neumann boundary conditions (3c) results in the following weak form:

$$\int_\Omega W \frac{\partial(\phi\rho_\alpha S_\alpha)}{\partial t}\,\mathrm{d}x + \int_\Omega \rho_\alpha\lambda_\alpha \nabla W \cdot K \cdot (\nabla p_w + \delta_{\alpha n}\nabla p_c - \rho_\alpha g)\,\mathrm{d}x, \tag{6}$$
$$= \int_{\partial\Omega_{Neu}} W\phi_\alpha\,\mathrm{d}S + \int_\Omega W\rho_\alpha q_\alpha\,\mathrm{d}x \qquad \alpha \in \{w, n\},$$

where $\lambda_\alpha \equiv \frac{k_{r\alpha}}{\mu_\alpha}$ stands for the α-phase mobility coefficient. Discretizing the primary variables p_w and S_n by linear Lagrange elements with linear basis functions N_i, and using the implicit Euler time discretization together with the mass lumping technique, the following discrete CVFE scheme can be derived (see [12, 13, 17])

$$\frac{[\phi\rho_\alpha S_\alpha]_i^{n+1} - [\phi\rho_\alpha S_\alpha]_i^n}{\Delta t_n} V_i = \sum_{j\in\eta_i} \lambda_{\alpha ij}^{n+1}\rho_\alpha^{n+1}\gamma_{ij}\,(\psi_{\alpha j}^{n+1} - \psi_{\alpha i}^{n+1}) + (\rho_\alpha q_\alpha)_i^{n+1}\,V_i + m_{\alpha i}^{n+1}. \tag{7}$$

Here, i and j denote nodes of a triangulation $\mathcal{T}$, η_i is the set of neighbours of the node i, Δt_n is the nth time-step, n is the time-level, $\psi_\alpha = p_w + \delta_{\alpha n}p_c - \rho_\alpha g z_j$ is the α-phase potential, $V_i = \int_\Omega N_i\,dx$, $\gamma_{ij} = -\int_\Omega \nabla N_i \cdot K \cdot \nabla N_j\,\mathrm{d}x$, and $m_{\alpha i}$ represents the finite-element discretization of the Neumann boundary conditions (3c). The mobility coefficient λ_α is weighted using the full upwind weighting, i. e.

$$\lambda_{\alpha ij} = \begin{cases} \lambda_{\alpha i} & \text{if } \gamma_{ij}(\psi_{\alpha j} - \psi_{\alpha i}) \le 0, \\ \lambda_{\alpha j} & \text{if } \gamma_{ij}(\psi_{\alpha j} - \psi_{\alpha i}) > 0. \end{cases} \tag{8}$$

The equations (7) together with the Dirichlet boundary conditions (3a) and (3b) make up a system of non-linear algebraic equations that is solved using the Newton method. This leads to solution of several linear systems with large sparse non-symmetric matrices in each time-step. These systems are solved using the BiCGStab method (see [20]) used with linear multigrid as a preconditioner. More details can be found in [17].

This scheme has been implemented in the language C using the numerical library UG (University of Heidelberg, see [1, 2, 3]) into a new numerical code called VODA. The numerical code has been verified on two 1-D problems with known (quasi-)analytical solutions – namely Buckley–Leverett ([9, 14]) problem which neglects capillarity and on the McWhorter–Sunada problem ([5, 11, 15, 16]) which includes capillarity. Results of the experimental convergence analysis can be found in [4]. Moreover, the code also offers several methods of treatment of heterogeneity interfaces. These methods have been verified and the results are covered in [6].

4. INFLUENCE OF CAPILLARY PRESSURE PARAMETERS ON PLUME MORPHOLOGY

We investigate influence of the parameters p_d, λ and S_{nr} on the plume morphology. As the reference problem we simulate incompressible two-phase flow in a vertical

Table 1. Parameters of the reference problem for the sensitivity analysis.

ρ_w	999.7	[kg m^{-3}]	λ	4.931	[-]	K	$2.26 \cdot 10^{-10}$	[m^2]
ρ_n	1516.6	[kg m^{-3}]	p_d	2549.83	[Pa]	ϕ	0.43	[-]
μ_w	$1.0 \cdot 10^{-3}$	[kg m^{-1} s^{-1}]	S_{wr}	0.1294	[-]	p_{w0}	hydrostatic	[Pa]
μ_n	$5.8 \cdot 10^{-4}$	[kg m^{-1} s^{-1}]	S_{nr}	0.25	[-]	S_{n0}	0.0	[-]

Table 2. Reference problem for the sensitivity analysis: boundary conditions.

left boundary	$p_{wD} = p_{w0}$	$S_{nD} = 0.0$
right boundary	$p_{wD} = p_{w0}$	$S_{nD} = 0.0$
top & bottom boundaries	$\phi_w = 0.0$	$\phi_n = 0.0$
top inlet boundary	$\phi_w = 0.0$	$\phi_n = -0.5$ [kg.m^{-2} s^{-1}]

2-D sand layer in a rectangular domain Ω of size 1.6×1.6 m, initially fully water-saturated. At both side boundaries hydrostatic water pressure distribution and zero non-wetting phase saturations are maintained whilst the top and bottom boundaries are impermeable for both phases except from the central part of the top boundary with length of 20 cm through which a dense non-aqueous phase liquid (DNAPL) is introduced into the layer under a constant flux. A non-wetting phase is used with density higher than water, and thus DNAPL will try to percolate down into the layer in the direction of gravity. The sand layer is assumed to be homogeneous in the entire domain. The exact values of all parameters are given in Tables 1 and 2.

The reference problem is solved on an unstructured triangular two-level mesh with fine level consisting of 2388 elements with 1254 nodes. We are interested in state of NAPL saturation in time $T = 30$ min, which is achieved in 20 regular time steps of size $\Delta t = 1.5$ min. Then, the computation is repeated with a modified value of some parameter (p_d, λ, S_{nr}). In every simulation, we use all data of the reference problems except from exactly one parameter that is increased or decreased by 1%, 5%, 10%, 20%, and 50% from its original value. For every parameter we thus have a reference solution and 10 solutions of the perturbed problems. Resulting DNAPL saturation distributions for the reference problem and for the extreme values of the examined parameters are presented in Figure 2. The constant NAPL flux boundary condition ensures that the same mass of DNAPL is injected into the soil in all simulations.

For a quantitative characterization of the plume morphology we use the first and second moments of the plume. Generally, the i,jth moment of the plume (in a 2-D plane x-z) is defined as

$$M_{ij} = \int_\Omega x^i z^j \phi(x,z) \rho_n S_n(x,z) \, \mathrm{d}x\mathrm{d}z. \tag{9}$$

Clearly, M_{00} is the total mass of NAPL inside Ω. The first-order moments M_{10} and M_{01} can be normalized to determine coordinates of the *center of mass* of the NAPL

plume in terms of the following formula

$$X_c = \frac{M_{10}}{M_{00}} \qquad Z_c = \frac{M_{01}}{M_{00}}. \tag{10}$$

The second-order moments can be normalized and centered with respect to the first-order moments to obtain *variances* of the DNAPL plume

$$\sigma_x^2 = \frac{M_{20}}{M_{00}} - X_c^2 \qquad \sigma_z^2 = \frac{M_{02}}{M_{00}} - Z_c^2, \tag{11}$$

which can be interpreted as a measure of DNAPL spreading around the center of mass of the plume in the directions of the corresponding axes. This method of characterization of the plume distribution using the first- and second-order moments of the plume has been used in evaluation of laboratory experiments e. g. in [19].

Values of X_c, Z_c, σ_x^2, and σ_z^2 were determined for the reference problem as well as for all perturbed ones, and are plotted against the relative change of the respective parameters in Figures 3 – 5. The results indicate that with increasing λ, the plume is getting longer and more narrow, while the converse holds true for the entry pressure p_d. Higher values of the residual NAPL saturation S_{nr} lead to a smaller plume expanding slower with higher NAPL saturation values. On the contrary, lower values of residual NAPL saturation lead to a larger more diffusive plume of lower saturation. Although the total NAPL mass is the same in all simulations, we see that the volume of the plume can be quite different for different residual NAPL saturations. From Figures 3 – 5 it can also be seen that the spread in the z-direction (direction of gravity) is more sensitive to the capillary pressure parameters than the spread in the x-direction. This can be explained by the fact that in the horizontal direction the capillarity is the only force driving the flow whereas in the vertical direction both forces, capillarity and gravity, are active.

The results confirm the hypothesis that the capillary pressure parameters are important parameters that determine the DNAPL plume morphology. From the capillary pressure parameters in question, the residual NAPL saturation S_{nr} turns out to be most sensitive parameter. This contrasts with our experience that it is the residual NAPL saturation S_{nr} whose values are usually not known and must be estimated (c.f. [17]).

ACKNOWLEDGEMENT

The work has been partially supported by the project "Applied Mathematics in Technical and Physical Sciences" MSM 6840770010, by the project "Environmental Modelling" KONTAKT ME 878, and by the project "Jindřich Nečas Center for Mathematical Modelling" LC06052, all of the Ministry of Education of the Czech Republic, and by the National Science Foundation through the award 0222286 (CMG RESEARCH: "Numerical and Experimental Validation of Stochastic Upscaling for Subsurface Contamination Problems Involving Multi-phase Volatile Chlorinated Solvents").

(Received November 30, 2006.)

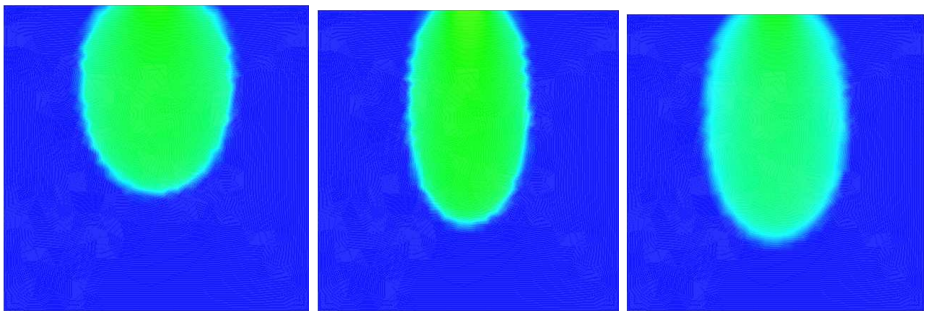

$\lambda = 2.4655$ $p_d = 1274.915$ Pa $S_{nr} = 0.125$

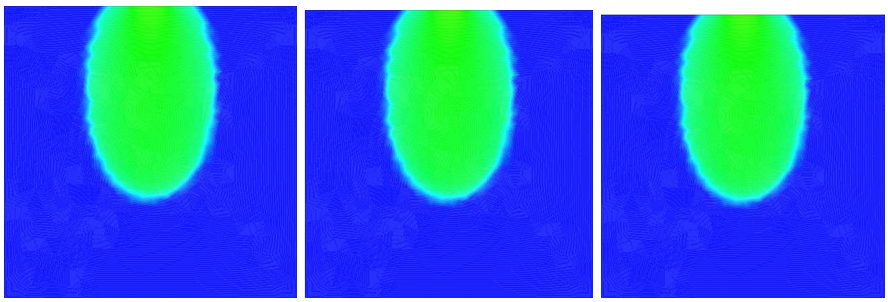

The common reference solution with $\lambda = 4.931, p_d = 2549.83$ Pa, $S_{nr} = 0.25$

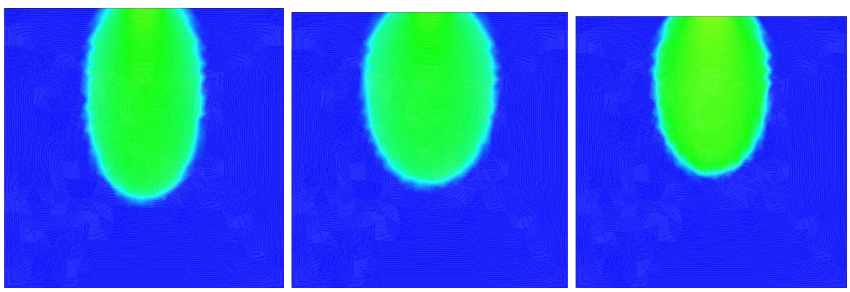

$\lambda = 7.3965$ $p_d = 3824.745$ Pa $S_{nr} = 0.375$

Fig. 2. DNAPL saturation distribution for different values of λ (left column), p_d (middle column), and S_{nr} (right column). The central row is the common reference solution. In the top row the each parameter is decreased by 50 % while in the bottom row it is increased by 50 % with respect to its reference settings. The dark backgrounds correspond to uncontaminated domains with $S_n = 0$, while the lighter shadows correspond to domains with positive values of NAPL saturations.

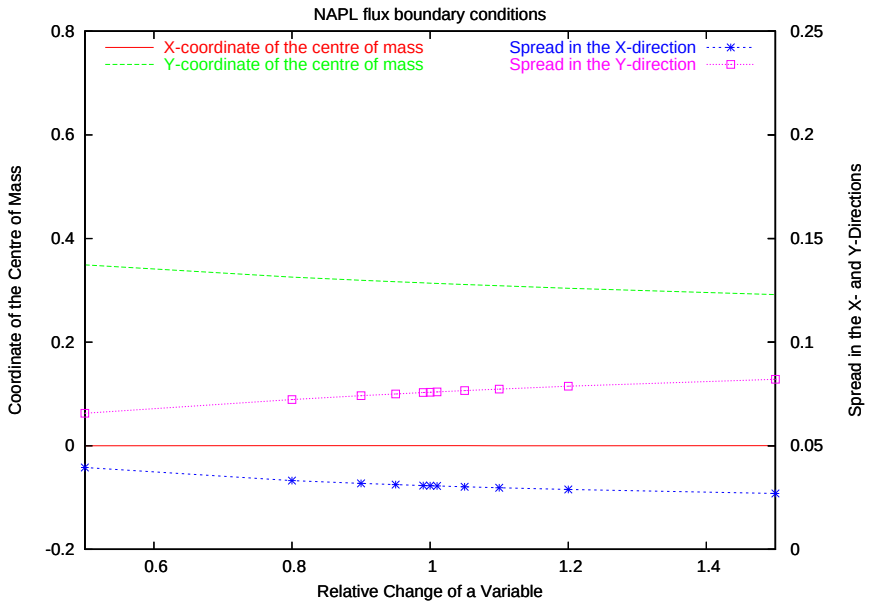

Fig. 3. Plot of the first- and second-order moments against the relative changes of Brooks–Corey parameter λ.

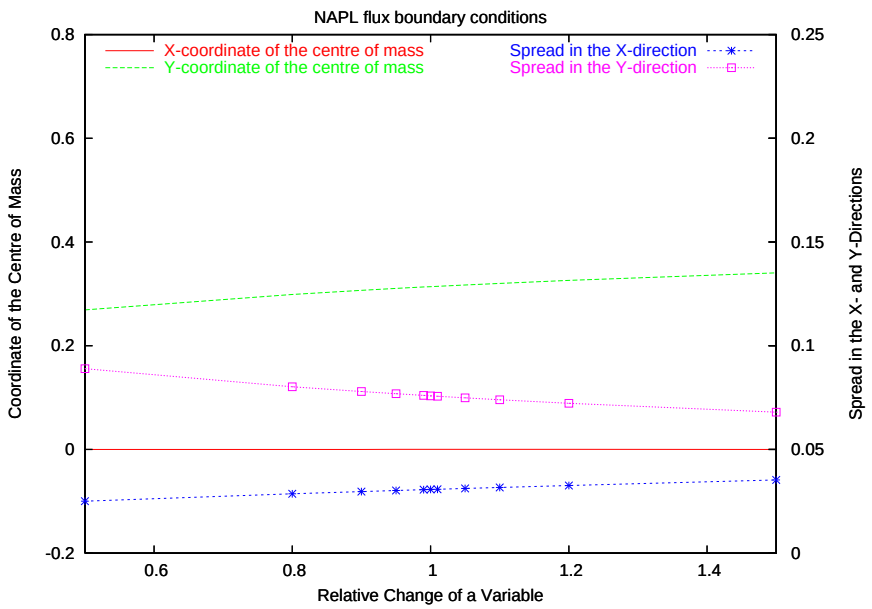

Fig. 4. Plot of the first- and second-order moments against the relative changes of entry pressure p_d.

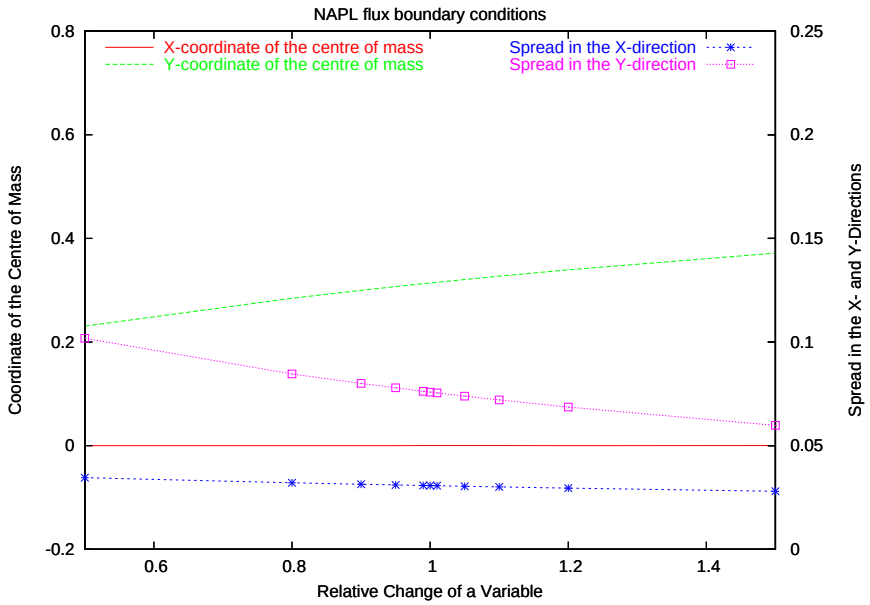

Fig. 5. Plot of the first- and second-order moments against the relative changes of residual NAPL saturation S_{nr}.

REFERENCES

[1] UG homepage. http://sit.iwr.uni-heidelberg.de/~ug/.

[2] P. Bastian, K. Birken, S. Lang, K. Johannsen, N. Neuß, H. Rentz-Reichert, and C. Wieners: UG: A flexible software toolbox for solving partial differential equations. Comput. and Visualization in Science *1* (1997), 27–40.

[3] P. Bastian, K. Johannsen, and V. Reichenberger: UG Tutorial, 1999.

[4] M. Beneš, R. Fučík, J. Mikyška, and T. H. Illangasekare: Generalization of the benchmark solution for the two-phase flow. In: FEM_MODFLOW 2004 (K. Kovář, Z. Hrkal, and J. Bruthans, eds.), Karlovy Vary 2004, pp. 181–184.

[5] M. Beneš, R. Fučík, J. Mikyška, and T. H. Illangasekare: An improved semi-analytical solution for validation of numerical models of two-phase flow in porous media. Vadoze Zone Journal *6* (2007), 93–104 . ISSN 1539-1663.

[6] M. Beneš, T. H. Illangasekare, and J. Mikyška: On the numerical treatment of sharp texture transitions in two-phase flow. In: Czech–Japanese Seminar in Applied Mathematics 2005 (M. Beneš, M. Kimura, and T. Nakaki, eds.), COE Lecture Note Vol. 3, Hakozaki 6-10-1, Higashi-ku, Fukuoka, 812-8581, Japan 2006, pp. 106–116. Available on-line at http://www.math.kyushu-u.ac.jp/ masato/cj/proceedings-CJ05.html.

[7] M. Beneš, M. Stýblo, J. Maryška, and J. Mužák: The application of mathematical models of the transport of chemical substances in the remediation of consequences of the uranium mining. In: Proc. 3rd Workshop on Modelling of Chemical Reaction Systems, Heidelberg 1996, ISBN 3-932217-00-4.

[8] R. H. Brooks and A. T. Corey: Hydraulic properties of porous media. Colorado State University Hydrology Paper *3*, Colorado State University 1964.

[9] S. E. Buckley and M. C. Leverett: Mechanism of fluid displacements in sands. Trans. AIME *146* (1942), 107–116.
[10] N. T. Burdine: Relative Permeability Calculations from Pore-size Distribution Data. Technical Report, Petroleum Transaction, AIME, 1953.
[11] Z. X. Chen, G. S. Bodvarson, and P. A. Witherspoon: Comment on "exact integral solution for two-phase flow" by David B. McWhorter and Daniel K. Sunada. Water Resources Research *28* (1992), 5, 1477–1478.
[12] P. A. Forsyth: A control volume finite element approach to NAPL groundwater contamination. SIAM J. Sci. Statist. Comput. *12* (1991), 5, 1029–1057.
[13] R. Helmig: Multiphase Flow and Transport Processes in the Subsurface: A Contribution to the Modeling of Hydrosystems. Springer Verlag, Berlin 1997.
[14] P. S. Huyakorn and G. F. Pinder: Computational Methods in Subsurface Flow. Academic Press, New York 1983.
[15] D. B. McWhorter and D. K. Sunada: Exact integral solutions for two-phase flow. Water Resources Research *26* (1990), 3, 399–413.
[16] D. B. McWhorter and D. K. Sunada: Reply. Water Resources Research *28* (1992), 5, 1479.
[17] J. Mikyška: Numerical Model for Simulation of Behaviour of Non-Aqueous Phase Liquids in Heterogeneous Porous Media Containing Sharp Texture Transitions. PhD Thesis, Faculty of Nuclear Science and Physical Engineering, Czech Technical University in Prague, Prague 2005.
[18] R. Straka: Numerical simulation of reaction-diffusion dynamics. In: Proc. Czech Japanese Seminar in Applied Mathematics (M. Beneš, J. Mikyška, and T. Oberhuber, eds.), Czech Technical University in Prague 2005.
[19] A. D. Turner: Behavior of Dense Non-aqueous Phase Liquids at Soil Interfaces of Heterogeneous Formations: Experimental Methods and Physical Model Testing. Master's Thesis, Colorado School of Mines, Golden, Colorado 2004.
[20] H. A. van der Vorst: Bi-CGSTAB: A fast and smoothly converging variant of Bi-CG for the solution of non-symmetric linear systems. SIAM J. Sci. Statist. Comput. *13* (1992), 631–644.

Jiří Mikyška, Czech Technical University in Prague, Faculty of Nuclear Sciences and Physical Engineering, Department of Mathematics, Trojanova 13, 120 00 Praha 2. Czech Republic.
e-mail: mikyska@kmlinux.fjfi.cvut.cz

Tissa H. Illangasekare, Center for Experimental Study of Subsurface Environmental Processes, Colorado School of Mines, 1500 Illinois St., Golden, CO 804 01. U. S. A.
e-mail: tissa@mines.edu